Iranian Journal of Chemical Engineering
Vol. 3, No. 2 (Spring), 2006, IAChE

Experimental Investigation of Power Consumption, Mass Transfer Coefficient and Flow Regime in Gas-Liquid Dispersion Systems

N. Saghatoleslami[1] and H. R. Bakhtiari[2]*
1- Deptartment of Chemical Engineering, University of Ferdowsi, Mashhad, Iran.
2- Research Institute of Petroleum Industry, Tehran, Iran.

Abstract
Gas liquid dispersion technology is a major part of the infrastructure of chemical, petrochemical and biochemical industries. Flooding is one of the characteristic features of stirred tank equipment used to disperse gases in liquids. Most investigators have studied the flow regime and mass transfer coefficient relying solely on the Rushton turbine. However, there are cases wherein the utilization of an inappropriate type of impeller results in both waste of energy and marked counter-productivity. Hence, the objective of this paper is to examine the performance of gas-liquid dispersion systems in terms of flow regime, mass transfer coefficient and the loading zone for the gassed condition using the Rushton turbine, pitched blade, concave blade and the vaned disc type impellers. For the gassed conditions, we concluded that the vaned type disc gives the optimal mass transfer coefficient. We have also examined the hysteresis phenomena for the Rushton turbine and established a new flow region called transition, in which both the loading and flooding zone is present.

Keywords: *Stirred vessels, Mass transfer coefficient, Hysteresis effect, Loading region, Flooding region*

Introduction
Several major operations, e.g., oxidation, hydrogenation and biological fermentations involve the contacting of gases and liquids. It is the objective of such processes to agitate the gas liquid mixture thus generating a dispersion of gas bubbles in a continuous liquid phase. Gas absorption is limited by the interfacial area and the liquid phase mass transfer. The interfacial area can be increased by mechanical agitation, which produces turbulence and shear forces to break up the gas in small bubbles. Different agitators behave in different ways. Thus, it is essential when designing a mechanical agitated gas-liquid system to select the most suitable agitator and adequate operating conditions, such as power and flow of gas, to achieve the highest mass transfer. An inappropriate choice of one of these parameters could cause an improper distribution of the gas throughout the reactor and, as a consequence of this, a poor mass transfer from the gas to the liquid. Consequently, in the design of such processes, the most important consideration is the interfacial contact as well as the mass

* - Corresponding author: E-mail: slami@um.ac.ir

transfer between phases. To enhance the rate of mass transfer, turbulence is created by the impeller which causes the resultant shear forces to break up the bubbles. Here, the choice of a proper impeller plays an important role on the required rate of mass transfer. Chapman, Nienow, Cooke and Middleton [1] investigated the effect of speed and power on gas-liquid mixing. Warmoeskerken and Smith [2] did a comprehensive study on the flooding of the Rushton turbine and obtained the following relation between the flow number (Fl) and Froude number (Fr):

$$Fl = \alpha \,.\, Fr \qquad (1)$$

where α is the constant of proportionality and a value of 1.2 is reported for it. This study was performed using a Rushton turbine and with a tank to impeller diameter ratio of 2.5. The transition between impeller loading and flooding was ascertained by means of a method based on qualitative determination of the liquid radial outflow vector near the impeller by a small propeller.

In a subsequent work [3], the same authors suggested a similar expression which includes the impeller to tank diameter ratio:

$$N_A = C_F \left(\frac{D}{T}\right)^{3.5} N_{Fr} \qquad (2)$$

where

$C_F = 70$ for a flat-blade impeller and

$C_F = 30$ for a concave-blade impeller

With this equation, Warmoeskerken and Smith argued that at the same speed and diameter, the concave blade type of the impeller can handle more than twice the gas flow rate of the flat type before being flooded. On the other hand, Tatterson [4] suggested that this discrepancy is due to the different shape of the blades, which leads to the formation of more vortices in the outer perimeter of the concave type of impellers. They argued that the concave impellers generate three vortices: one vortex forms inside the cup and two vortices along the top and bottom edges of the blades.

The Rushton turbine develops only two vortices along the top and bottom part of the blade, respectively. Liquid pumping in the concave type impellers cropped up both from the front and back while this only appeared from the back side in the Rushton type of impellers. As a consequence of this, the concave type of impeller can disperse the liquid and the gas in a much more efficient way than the Rushton turbine type of impellers.

When gas is added to an agitated vessel, it causes the power demand to drop off. This is partly due to the fall of density of the solution and partly to the reduction in resistant force caused by the development of gas cavities behind the impeller blade. This effect has to be taken into account when designing a gas liquid system to prevent the motor from overloading when the gas flow is interrupted. An effective way to quantify the drop in power demand is to evaluate the ratio of the power draw to the unaerated power draw [5 and 6]. An empirical correlation for this ratio is:

$$\frac{P_g}{P_u} = 1 - (b - a\mu) N_{Fr} \tanh(cN_A) \qquad (3)$$

where P_u is the power under ungassed conditions, N_A is the aeration number, N_{Fr} is the Froude number and a, b and c are constants.

The effect of the height of liquid on transition from loading (i.e., favorable distribution of bubbles) to the flooding region (i.e., the air is

poorly dispersed with no radial flow pattern [7]) has received some attention by Hudocova and Nienow [8]. At high gas loadings, the impeller no longer pumps the gas and liquid mixture adequately and the gas bubbles rises axially to the liquid surface. They concluded that there is a distinguishable boundary for transition from the loading to the flooding region.

Therefore, it is the objective of this précis to scrutinize the performance of gas-liquid dispersion systems in terms of the flow regime, mass transfer coefficient and the loading zone for the gassed condition using the Rushton turbine, pitched blade, concave blade and vaned disc type of impellers and to examine the hysteresis phenomena for the Rushton turbine.

Experimental Set-up and Procedure

A perspex cylindrical vessel which was fitted with four baffles of an inside diameter of 0.18 m was utilized in this work (as shown in figure 1). Also for simplicity, dry air (filtered) and water were chosen as the working fluid in this analysis. A sparger with a diameter of 0.8 m was employed for the distribution of the gas phase [9]. Moreover, four different types of impellers (i.e., Rushton turbine, pitched blade, concave blade and vaned disc) with a diameter equivalent to 40% of vessel diameter were scrutinized in this study. To ensure accuracy, gas flow rates were corrected for the operating temperature and pressure of the testing conditions. To measure the speed of the agitator, a tachometer was attached to the motor. The vessel was also equipped with an electric motor of 900 watts power. In order to estimate the power consumption, a digital voltmeter and ammeter were utilized. Also, during each test run the concentration of oxygen in water was evaluated by an oxygen electrode. In addition, to diminish the oxygen content of the solution before each test run, nitrogen was first introduced into it. Moreover, to compare the volumetric coefficient of mass transfer for the impellers used, concentration of oxygen in the solution at various time intervals (i.e., 5 seconds) were evaluated.

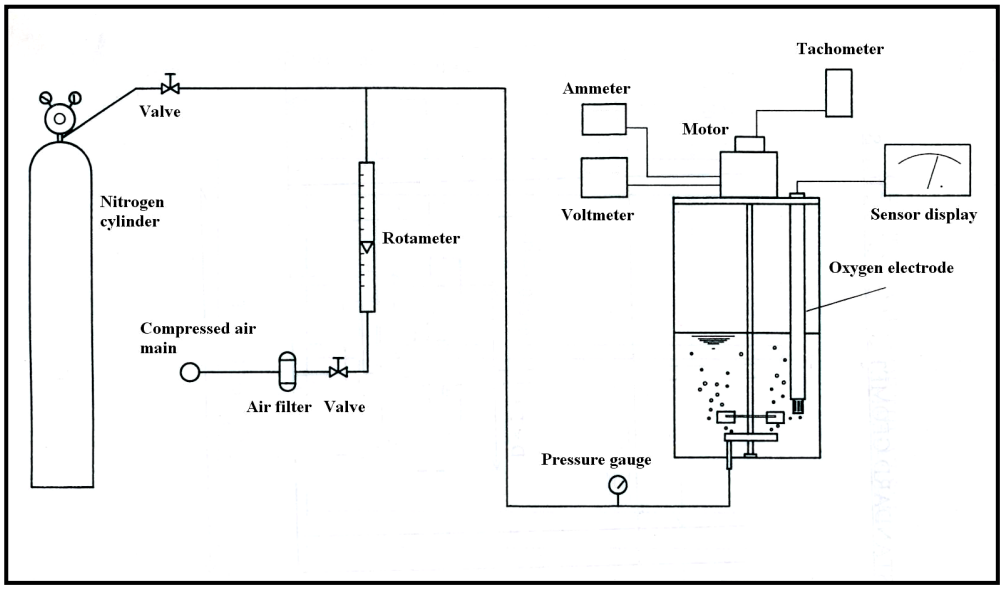

Figure 1. Schematic flow diagram

The mass transfer coefficient ($K_L a$) for oxygen is considered to be a useful way of characterizing bioreactors in aerobic processes. The volumetric oxygen transfer coefficient, $K_L a$, is defined by the reciprocal value of the liquid resistance, related to the system volume and multiplied by the total interfacial area between the gas and liquid phase. The rate of oxygen transfer (i.e., MTR) is given by the coefficient of oxygen transfer multiplied by the total area of dispersion and by the mean driving force which is given by:

$$MTR = K_L A \ \Delta C_{mean} \quad (4)$$

For a well mixed reactor:

$$MTR = K_L A \left(C_E - C_L\right) = \frac{d C_L}{d t}\left(V_L\right) \quad (5)$$

The overall rate oxygen transfer (i.e., MTR^*) is given by the following equation:

$$MTR^* = K_L a \left(C_E - C_L\right) = \frac{d C_L}{d t} \quad (6)$$

where C_E is the apparent mean oxygen concentration in the liquid which is in equilibrium with the oxygen concentration in the gas phase, C_L the concentration of the dissolved oxygen at arbitrary time, A is the total interfacial area, V_L is the volume of the tank and a is the interfacial area per unit volume. The equilibrium concentration C_E is usually calculated from Henry's law.

To determine the volumetric oxygen mass transfer coefficient, two techniques are available:

- The Dynamic Gassing-in Method
- The Sulfide Method

In this work, the dynamic gassing-in method was implemented. The popularity of the gassing-in method is due to its simplicity and relative accuracy. This process is based on measuring the rate of change of dissolved oxygen concentration in the liquid when aerated, following its deoxygenation, usually by nitrogen. The dissolved oxygen is measured by means of an oxygen electrode probe. The dependence of the dissolved oxygen with time is given by the equation:

$$N_a = \frac{dC_L}{dt} = K_L a \left(C_E - C_L\right) \quad (7)$$

The integration of this equation in the range C_L^0 to C_L and t_0 to t using the assumption of constant $K_L a$ and C_E gives [10]:

$$K_L a = \left(\frac{1}{t - t_0}\right) \ln \frac{C_E - C_L^0}{C_E - C_L} \quad (8)$$

By plotting the logarithmic part of the equation versus time, one can evaluate the volumetric mass transfer coefficient (i.e., $K_L a$) which is the slope of the straight line. During each test run provision has been made to stop the reading, if the rate of oxygen concentration remained unchanged.

Results and Discussion

Figure 2 demonstrates the concentration of oxygen versus time for an impeller of the concave type with a fixed flow rate, agitator speed and power consumption (i.e. 1724 W/m^3). The result reveals that as time increases (up to a limit), the concentration increases accordingly. However, about t=70s, the curve becomes almost asymptotic.

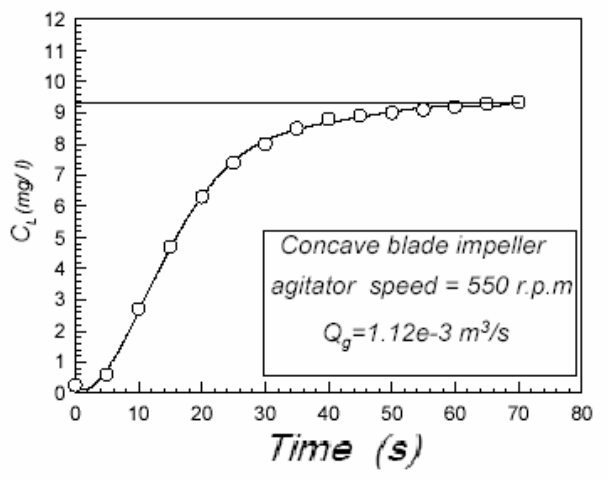

Figure 2. Concentration variation of O_2 with time

By applying equation 3, a graph of $\ln\left(C_E - C_L^0 / C_E - C_L\right)$ against time for each type of impeller and for a fixed operating condition can be plotted. From which, the mass transfer coefficient (i.e., the slope of the straight line) as shown in figure 3 can be evaluated. Figures 4a and 4b exhibit the variation in the mass transfer coefficient with the flow rate, for different types of impellers (keeping the agitator speed constant). It is evident from these figures that the vaned disc type of impeller has the highest mass transfer coefficient at analogous circumstances (in contrast with the other types adopted in this work). Figure 4a also reveals that for the Rushton type of impeller and for a given value of rpm, a gas flow rate exits (i.e, about 0.00085 m^3/s) over which a drop in the volumetric mass transfer coefficient (i.e., K_La) is observed that is caused by flooding [11].

Further tests were carried out for the Rushton type of impeller, in order to find a coherent relation for the hysteresis effect between transition from the loading to the flooding region and vice versa. Even though many investigators have worked on this phenomenon, they have not reported a region where both the loading and flooding region can be stable. As shown in figure 5, with an increase in power, the speed of the impeller will also increase accordingly up to the maximum value of N_{F+} (for a fixed gas flow rate of 1.66×10^{-4} m^3/s) and then a sharp decline in power is observed next to this point. However, from then on if we attempt to increase the impeller speed further, power will decline up to a minimum value and from then on a sharp rise in power will be observed. However, to reverse the process by reducing the speed, the result will only be reproducible up to a limit (i.e., N_{F+}). With further reduction of impeller speed, hysteresis occurs which diminishes after a certain speed (i.e., less than N_{F-}).

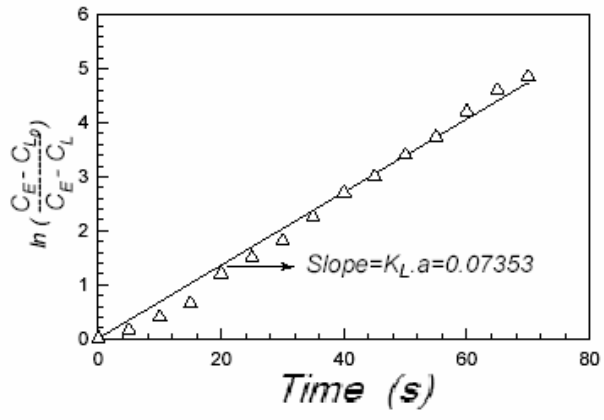

Figure 3. Mass transfer coefficient estimation

Furthermore, the hysteresis effect can also be observed for a fixed agitator speed. In figure 6, at a fixed value of impeller speed, abrupt changes of power with gas flow rate can be observed. However, reversing the process by means of reducing the gas flow rate, will result in a different value for the power. The area enclosed between these two curves exhibit the area in which both the flooding and loading phenomenon can occur for a fixed impeller speed. In this region both flooding and loading will also be stable.

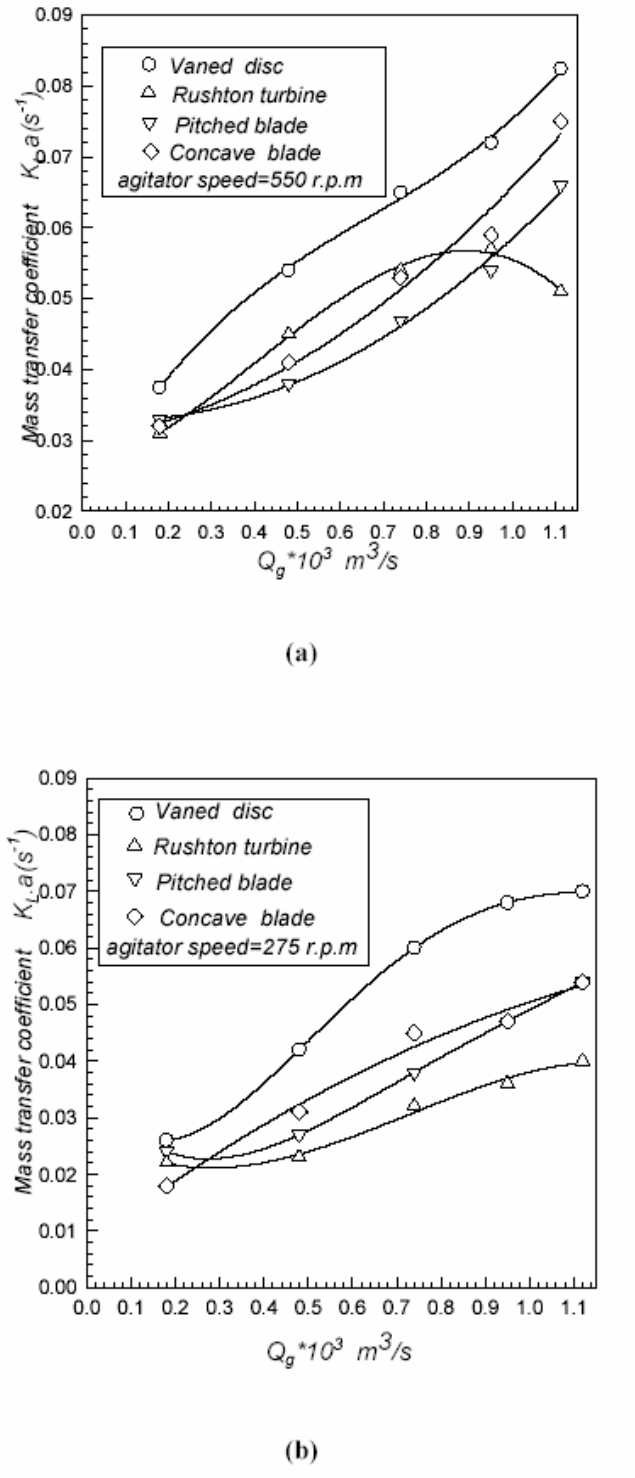

Figure 4. Comparison of mass transfer coefficients at a) high and b) low agitator speeds

The effect of geometric configurations of the vessel on the hysteresis phenomenon have also been studied in this work. Figure 7 reveals that as the head of water above the agitator (i.e., H-C) becomes larger than 0.045 m, the difference between critical speeds (i.e., N_{F+} and N_{F-}) increases accordingly. In addition, for a fixed flow rate of 2.15×10^{-4} m^3 and $(H-C)/T \rangle 0.25$, the flooding zone will tend to decrease. Figure 8 shows that the vaned and concave type of impellers have a larger transition zone than the pitched blade which can be influenced by the formation of a cavity behind impeller blades [12, 13].

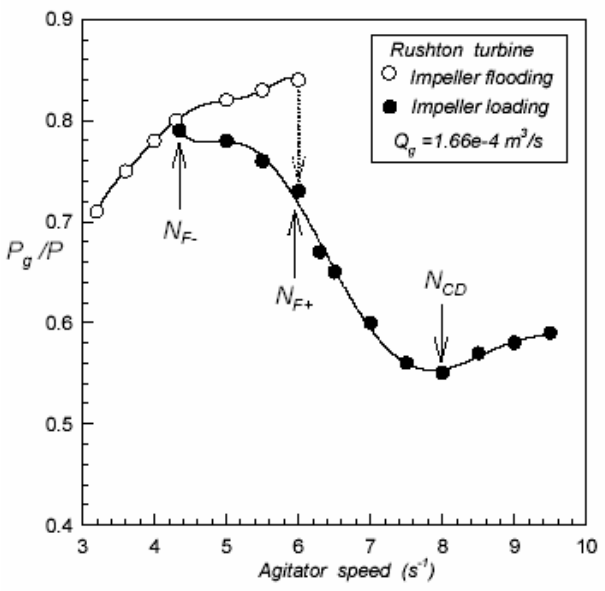

Figure 5. Hysteresis effect at low gas flow rate

In the Rushton turbine, a region exists where both the flooding and loading phenomenon are observed [10]. Experiments have been carried out in order to plot the flow number versus the Froude number for Rushton type impellers by taking into account both the loading and flooding region and specifying the transition boundaries. To obtain this objective, in regions where both loading and flooding exists, a pair of critical speeds have been recorded for a fixed gas flow rate and the Froude number has been calculated for a

given speed. As shown in figure 9, the transition region exists for a low gas flow rate (Fl < 0.04) and the extent of this zone is significant; however as the flow rate increases (i.e., Fl > 0.17) this region tends to diminish and can be discarded. The flow number relative to the Froude number has also been plotted on the same figure in accordance with the following equation:

$$\frac{Q_g}{N D^3} \propto \frac{N^2 D}{g} \qquad (9)$$

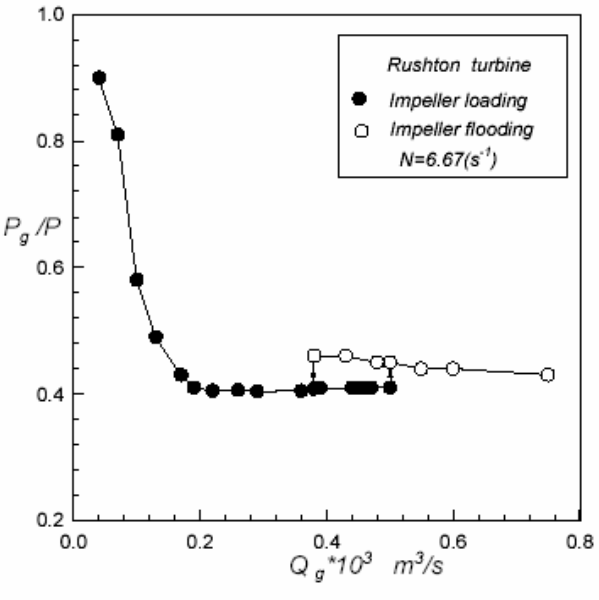

Figure 6. Hysteresis effect for a fixed agitator speed

This result means that the flooding transition should be described by a linear relation between the gas flow number and Froude number. The proportionality constant was found to be 1.2 [2]. Thus the relation describing the flooding transition becomes:

$$Fl = 1.2\,Fr \qquad (10)$$

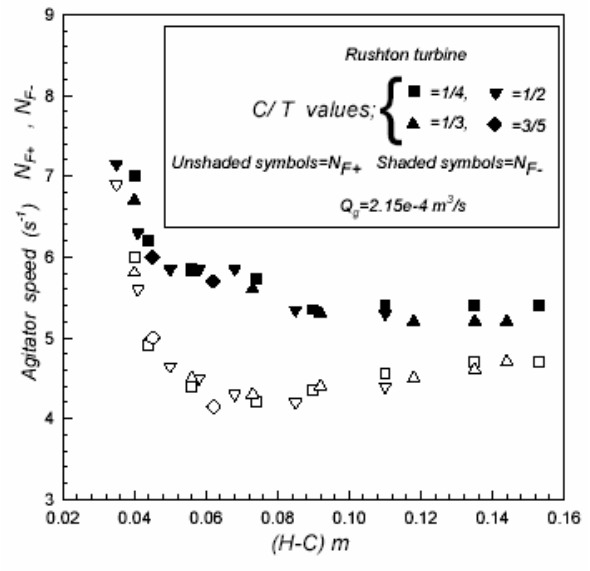

Figure 7. Effect of (H-C) on the hysteresis phenomenon

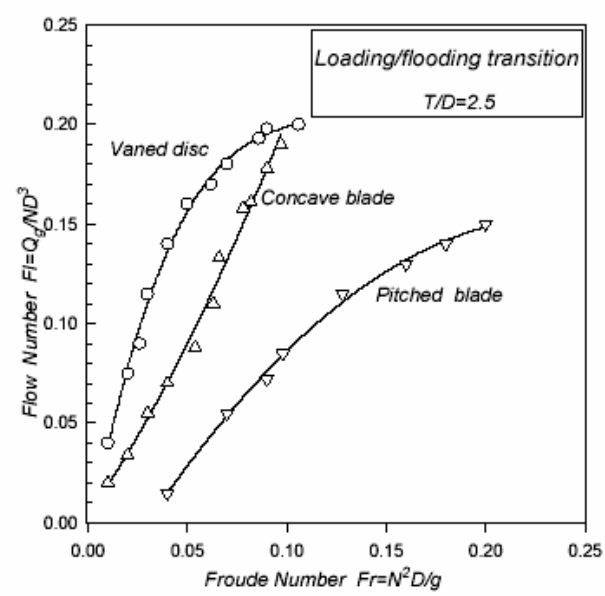

Figure 8. Flow regime for different types of impellers

It is worth noting that in the work of Warmoeskerken and Smith [2] they have not taken into account the region where both loading and flooding exist (i.e., Fl < 0.17). They have only extrapolated their values for

the low gas flow rate. Figure 9 reveals a high flow number (i.e., Fl > 0.17), the result of present work and Warmoeskerken and Smith [2] are in agreement with a high degree of concurrence.

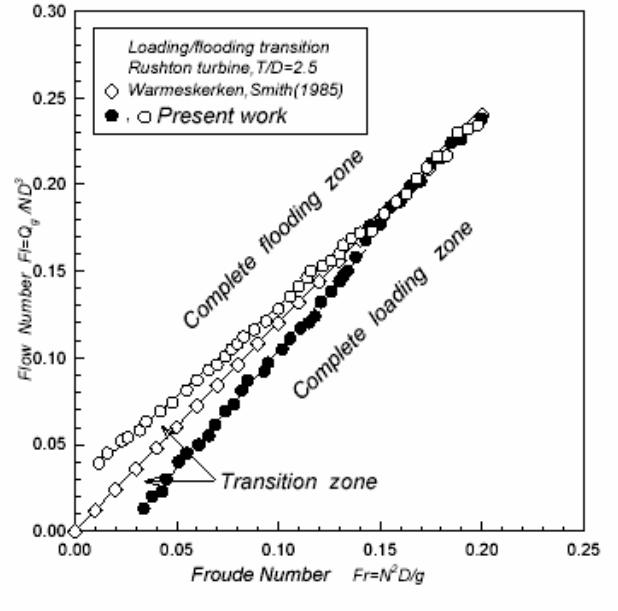

Figure 9. Comparison of the flow regime boundaries of the present study with the experimental data of [2]

The experimental data from this work has been fitted linearly and the resulting equations from the above regression and for different gas flow rates, indicates the following flow regime was predicted and plotted in figure 10 and compared with the experimental data of the present work:

a) For a low gas inlet flow rates
(i.e., Fl < 0.17):

- In the case where:

$$\mathrm{Fl} > 0.02555 + 1.4064\,(\mathrm{Fr})$$

Then the flooding flow regime exists.

- In the case where:

$$\mathrm{Fl} < -0.032552 + 1.3615(\mathrm{Fr})$$

Then the loading flow regime exists.

- In the case where:

$$\mathrm{Fl} > -0.032552 + 1.3615(\mathrm{Fr})$$

Then the transition flow regime exits.

b) For a higher gas inlet flow rates
(i.e., Fl > 0.17):

- In the case where:

$$\mathrm{Fl} > 2.917\times10^{-3} + 1.18075\,(\mathrm{Fr})$$

Then the loading flow regime exists.

- In the case where:

$$\mathrm{Fl} > 5.464\times10^{-3} + 1.17035\,(\mathrm{Fr})$$

Then the flooding flow regime exists.

- In the case where:

$$\mathrm{Fl} < 2.917\times10^{-3} + 1.18075\,(\mathrm{Fr})$$

and

$$\mathrm{Fl} > 5.464\times10^{-3} + 1.17035\,(\mathrm{Fr})$$

Then the transition flow regime exists.

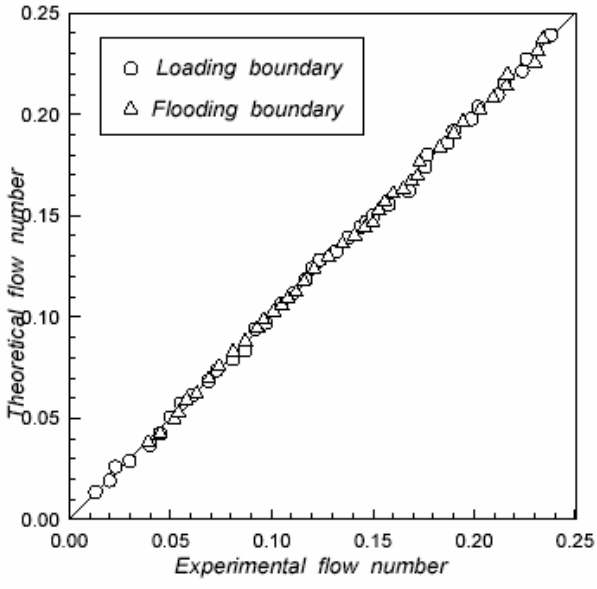

Figure 10. Comparison of the experimental data and the fitted equations obtained from this study

It is evident form figure 9 that even though there exists some discrepancy between the experimental data obtained by Warmoeskerken and Smith [2] and the present work for flow numbers less than 0.17, nevertheless for higher flow numbers the results of the present work is compatible

with those of Warmoeskerken and Smith [2]. The above discrepancy can be explained by the fact that Warmoeskerken and Smith [2] have discarded the transition region for flow numbers less than 0.17. Furthermore, figure 10 also reveals that the experimental data superimpose well with the fitted equations obtained from the present study. Therefore, theses equations can be used safely to predict the above flow regime in the Rushton type of impellers with a high degree of accuracy.

Conclusion

Experimental results reveal that the vaned disc type of impellers give the best outcome in terms of mass transfer coefficient and the extension of the loading region. Therefore, for an identical operating condition, the mass transfer coefficient becomes larger, the volume of the reactor will be reduced and hence a higher volume of gas will be dispersed before loading can occur.Thus, the vaned disc type of impeller would be an excellent replacement for the commonly used Rushton turbine and can substantially reduce the overall cost. Moreover, the result of this work also determined that the transition region for the Rushton turbine type of impellers can only be discarded for higher flow numbers (Fl 〉 0.17).

Acknowledgment

We gratefully acknowledge the support of the Research Institute of Petroleum Industry in Tehran, and in particular Mr. S. Sadraei.

Nomenclature

C agitator clearance from base, m

C_E concentration of oxygen in water, mol/m^3

C_L concentration of oxygen in water at time t, mol/m^3

C_L^0 concentration of oxygen in water at t = 0 , mol/m^3

D overall agitator diameter, m

Fl flow number, Q_g/ND^3 (dimensionless)

Fr Froude number, N^2D/g (dimensionless)

H height of liquid

K_La volumetric mass transfer coefficient, m/s

N agitator speed, rev s^{-1+}

N_A Aeration number, Q_g/ND^3 (dimensionless)

N_{CD} minimum speed to completely disperse the gas, rev s^{-1}

N_{F+} critical transition region speed with an increasing trend of agitator speed, s^{-1}

N_{F-} critical transition region speed with a decreasing trend of agitator speed, s^{-1}

P ungassed agitator power consumed by liquid**,** W

Pg agitator power consumed by gassed liquid, W

P_u agitator power consumed by ungassed liquid, W

Qg mean gas volumetric throughput rate, m^3/s

t time, s

T vessel diameter, m

References

1. Chapman C. M., Nienow A. W., Cooke M., and Middleton J. C., “Particle gas-liquid mixing in stirred vessels”, *Chem. Eng. Res. Des.*, **61**, 82 (1988).
2. Warmoeskerken M. M. C. G., and Smith J. M., “Flooding of disc turbines in gas-liquid dispersions”, *Chem. Eng. Sci.*, **40**(11), 2063 (1985).
3. Warmoeskerken M. M. C. G., and Smith J. M., “The hollow blade agitator for dispersion

and mass transfer", *Chem. Eng. Res. Des.*, **67**, (1989).

4. Tatterson, G. B., Scale-up and design of industrial mixing processes, McGraw-Hill Inc., UK, (1994).
5. Sesel M. E., Myers K. J. and Fasano J. B., "Gas dispersion at high aeration rates in low to moderately viscous newtonian liquids", *AIChE Symposium Series*, **293**(89), pp. 76-84 (1992).
6. Bowers R. H., I.C.I. engineering research manual, Preliminary issue, (1955).
7. McDonough R. J., Mixing for the process industries, Van Nostrand Reinhold, New York, USA, (1992).
8. Hudocova V., and Nienow A. W., "On the effect of height of liquid on the loading-flooding transition", *Chem. Eng. Sci.*, **42**(2), 375 (1987).
9. Joshi J. B., and Rewatkar V. B., "Role of sparger design on gas dispersion", *Canadian J. Chem. Eng.*, **71**, 287 (1993).
10. Sherwood T. K., and Pigford T. K., Absorption and extraction, McGraw-Hill, New York, USA, (1952).
11. Oldshue J. Y., Fluid mixing technology, McGraw-Hill, New York, USA, (1972).
12. Khopkar A. R., Rammohan A. R., Ranade V. V. and Dudukovic, M. P., "Gas-liquid flow generated by a rushton turbine in stirred vessel: CARPT/CT measurement and CFD simulation", *Chem. Eng. Sci.*, **60**, 2215 (2005).
13. Smith J. M., "Gas-liquid dispersion" *I. ChemE Symposium*, 73, J13 (1982).